Numerical microstructure prediction for an aluminium casting and its experimental validation

***Unterreiter Guenter[1], Ludwig Andreas[2] and Wu Menghuai[2]**

(1. Materials Center Leoben Forschung GmbH, Leoben, Austria; 2. Chair for Simulation and Modelling of Metallurgical Processes, Department of Metallurgy, University of Leoben, Leoben, Austria)

Abstract: Virtual manufacturing based on through-process modelling becomes an evolving research area which aims at integrating diverse simulation tools to realize computer-aided design, analysis, prototyping and manufacturing. Numerical prediction of the as-cast microstructure is an initial and critical step in the whole through-process modelling chain for engineering components. A commercial software package with the capability of calculating important microstructure features for aluminium alloys is used to simulate a G-AlSi7MgCu0.5 laboratory casting. The simulated microstructure, namely grain size, secondary dendrite arm spacing and diverse phase fractions are verified experimentally. Correspondence and discrepancies are reported and discussed.

Key words: numerical microstructure prediction; aluminium casting; through-process modelling
CLC number: TG146.21/TP391.99 Document code: A Article ID: 1672-6421(2011)03-331-06

Shape casting is one of the most economically beneficial methods for producing high performance aluminium components in automotive and aerospace industries. However, unlike forging or other thermomechanical processing routes, the mechanical properties and performance of cast components are strongly dependent on the as-cast microstructure [1]. Majority of casting processes operate in the range of cooling rates between 0.1 and 20 $K \cdot s^{-1}$ [2]. The influence of the cooling rate on the solidification process of alloys was investigated by many authors [3-4]. Referring to their work increasing the cooling rate refines the microstructural features like secondary dendrite arm spacing, grain size and intermetallic phases [5]. Due to the varying wall thickness of the component the cooling rates at different sections are different. This leads to an inhomogeneous microstructure. Furthermore, different casting defects, such as porosity may form during solidification and be distributed unfavourably [6]. The in-homogeneously distributed microstructure and defects are sometimes destructive for the components. For example, the secondary dendrite arm spacing (SDAS) and the near-surface pores influence ultimately the fatigue life of the cast components. Such kind of inhomogeneity is not easily taken into account during the design, and usually a homogenous material is assumed. It implies that the mechanical properties and performance of the designed component might be overestimated. Therefore, there is a great demand for simulation tools which can be used by designers to predict the microstructure such as grain size, SDAS, etc. Moreover, the same tools can be integrated in the through-process simulation chain to optimize the whole manufacturing process virtually [6]. The current paper focuses on the validation of the casting simulation tool MAGMASOFT, by direct comparison of some simulation results with the experimental examinations.

***Unterreiter Guenter**

Male, born in 1971 in Austria. In 1999 he started studying ceramics at the University of Leoben. In 2007 he obtained his master's degree in engineering. In 2006 he joined the chair of modelling and simulation of metallurgical processes at the University of Leoben as a staff member. Since 2008 he is a doctoral candidate and is also working at the Materials Center Leoben (MCL). The research program of the MCL focuses on the integrated simulation of materials and components across the entire supply chain and on all length scales. The research interests of Unterreiter Guenter are mainly focused on numerical simulation of casting processes and virtual manufacturing based on through process models of aluminium castings. In the aforementioned topics, the data transfer between different simulation software packages (CFD, FEM, FDM) is a major part of the work.

E-mail: guenter.unterreiter@unileoben.ac.at

Received: 2011-07-28; Accepted: 2010-08-20

1 Material and experimental procedure

In order to investigate the influence of the cooling rate on the as-cast microstructure, 65 castings with a configuration of a step geometry shown in Fig. 1 (thicknesses 4, 6, 10, 16 mm) were poured and solidified in a steel die mould. The dies, consisting of fixed and removable parts, were cooled by a coolant (T = 285℃), with continuously cycles through the cooling channels. Commercial G-AlSi7MgCu0.5 aluminium alloy was used (Table 1). The melt was prepared in an electric resistance furnace and the pouring temperature of the melt was taken to be 720±10℃. Each melt was degassed for 440 s with a rotary degassing equipment using nitrogen as inert gas. For the quantification of the amount of dissolved hydrogen in the aluminium melt, the reduced pressure test or Straube-Pfeiffer technique was used [7]. The outcome of the Straube-Pfeiffer-Test was a density index (DI) of 0.5 which is a common value for industrial components like cylinder heads.

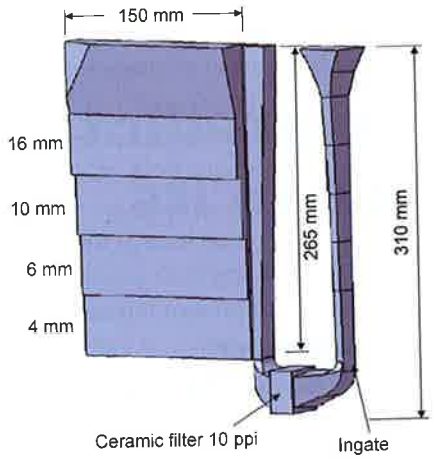

Fig. 1: Configuration of casting geometry (step plate)

Tab. 1: Alloy composition of AlSi7MgCu05 (wt.%)

Si	Fe	Cu	Mn	Mg	Zn	Sr	Ti	Al
7.0	0.12	0.49	0.071	0.42	0.014	0.024	0.11	Bal.

The castings were made in batches. Each casting cycle started with mould filling which took 7 s. After 100 s the movable die was opened, and both casting and die were continuously cooled in normal ambient temperature. The casting was finally removed from the mould after another 110 s. With ca. 10 s of delay the mould was closed again and the casting cycle repeated. It means each cycle took ca. 227 s.

Some sections of the present casting were designed to have different thicknesses. Hence, each step of the plate has its own cooling characteristics. A very critical parameter is the heat transfer coefficient (HTC) between mould and casting. This parameter influences the temperature distribution inside the domain and thus is affecting the cooling rate. For estimation of the order of the HTC the mould was instrumented with four thermocouples (TCs) of K-type. The TCs in the mould had a distance of five millimetres from the casting-mould interface (TC9 – TC12 in Fig. 2). The temperature data (T–t curves) were recorded with a data logger every ten seconds. Also a set of five castings were instrumented with K-type TCs which were positioned in the middle of each step (TC1 – TC4 in Fig. 2). The cooling curves in the casting were recorded every half second.

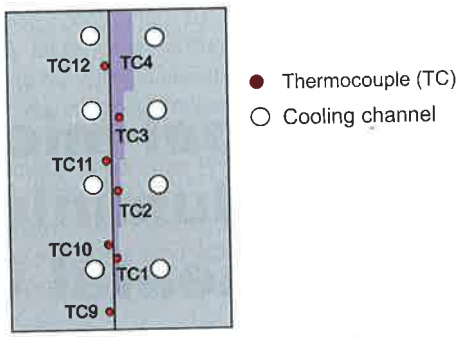

Fig. 2: Cross section of casting and mould
(Position of eight thermocouples (TC 1 – 4, TC 9 – 12) and eight cooling channels are shown)

The casting simulation consists in calculating the flow and temperature distributions during mould filling and the subsequent solidification process. In this work the commercial casting software MAGMASOFT Version 4.6 DP07 was used. This version offers a module of microstructure modelling for aluminium alloys. This advanced module allows, amongst others, to simulate the microstructure formation together with the resulting mechanical properties like yield strength, tensile strength and elongation. For the microstructure module the alloy composition in details and the enthalpy curve as a function of temperature are requested as additional input data. For example, the content of Ti, a critical element for grain refinement, is taken into account for calculating the grain size. The main focus in this work is on the calculation of features of the microstructure like secondary dendrite arm spacing (SDAS), grain size, the phase fractions of diverse ferrous phases and Mg_2Si.

The whole calculation domain was meshed with 1 309 280 Hexahedral Cells. For the mould filling process laminar flow of the melt was assumed. The measured temperature curves were used to determine a temperature-dependent HTC reversely. The finally optimized HTC as function of temperature is shown in Fig. 3(a). With this HTC the simulated temperature curves showed acceptable agreement with the temperature measurements , as shown in Fig. 3(b). The difference between measured and calculated temperatures of the TC 9 is probably due to the shrinkage of the casting and the subsequent displacement between TC and the surface of the casting.

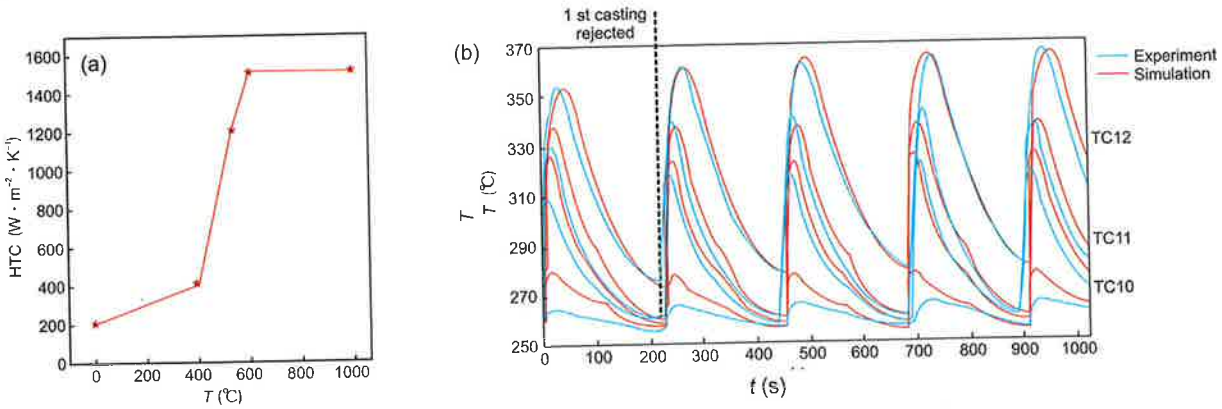

Fig. 3: (a) Temperature dependent heat transfer coefficient at mould – casting interface; (b) Comparison of measured and simulated temperatures curves of thermocouples 9–12

2 Results and discussion

Grain size and its morphology, the secondary dendrite arm spacing, size and distribution of secondary phases are key parameters, which determine mechanical properties of casting parts [8-9]. The as-cast step plate was cut into five parts (A – E) vertically (Fig. 4). From every part four metallographic samples (one each step) were taken and analysed with an Olympus BX51M light optical microscope. The average value of the SDAS was determined by the standard intercept count method [10]. Thereby 20 individual readings were taken on each metallographic sample. This yielded the SDAS-distribution throughout the plate. In Fig. 5 the calculated SDAS in the cutting planes A – D and Steps 1 – 4 is compared with the simulated SDAS. The variation of the measured data within a step can be explained by the measurement method. The observation of the SDAS was performed on planar sections through the material. Hence, the three dimensional dendrites were cut by a cutting plane and only the two dimensional features of the dendrites in the cross section were measured. This causes scattered measurement results (Fig. 5). Another reason for the differences could be that all surfaces which are in contact with the mold were assumed to have the same HTC. This simplification can lead to an error concerning the cooling rate because it is supposed that step 4 has a higher HTC than step 1.

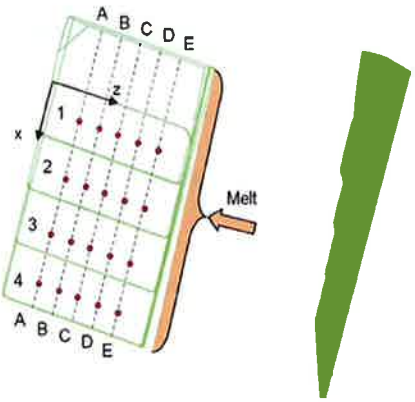

Fig. 4: Cutting plane and location of samples for measuring the SDAS

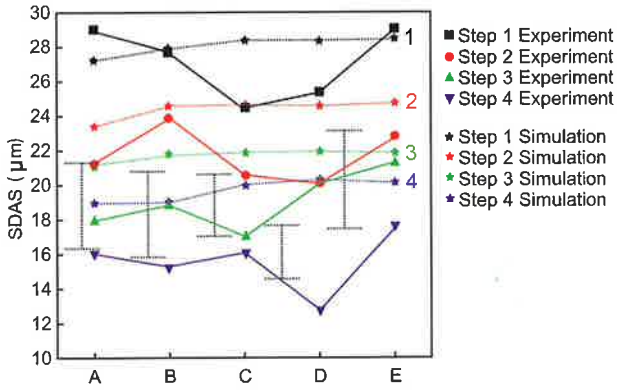

Fig. 5: Comparison of measured and simulated SDAS in the centre of steps 1, 2, 3, 4 with wall thickness 16, 10, 6, 4 mm corresponding

Furthermore the hot melt started to fill the mould from the bottom right corner, and so the temperature distribution is not symmetrical (Fig. 6), resulting in non-symmetrical cooling conditions which are also affecting the microstructure formation.

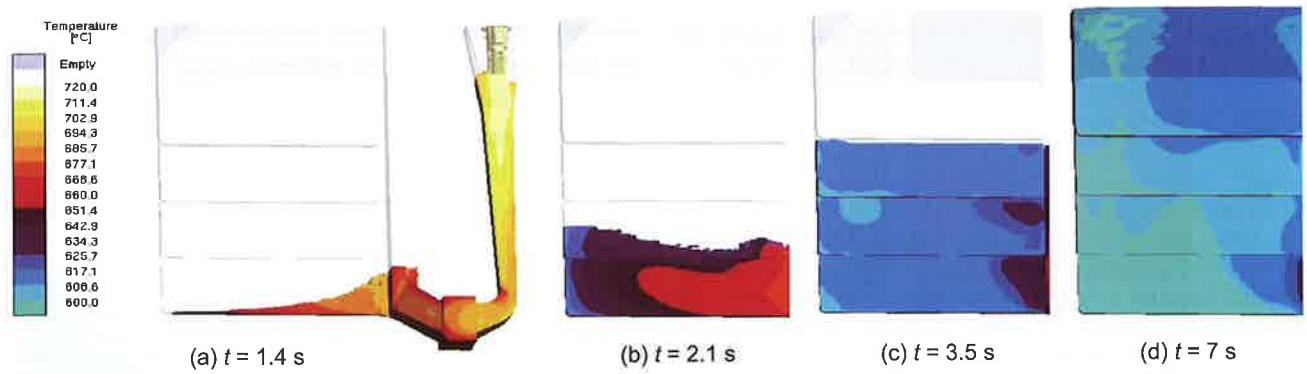

Fig. 6: Temperature field during mould filling sequence

In Fig. 7 the cooling rate after mould filling and the subsequent solidification process is shown. Equation 1 [11] is a well established relationship between the cooling rate and the dendrite arm spacing where A and n are alloy dependent parameters and V is the cooling rate in K·s^{-1} [12].

$$SDAS = A \cdot V^{-n} \qquad (1)$$

According to Equation 1 the SDAS decreases if the cooling rate increases, so a higher HTC at the 4 mm step would cause a reduced SDAS in the simulation results.

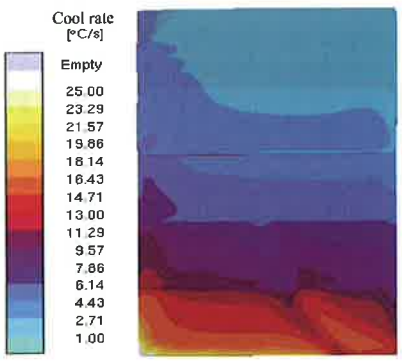

Fig. 7: Cooling rate between liquidus and solidus temperature in K·s^{-1}

Although the measured data of SDAS varies more within a step, the predicted and the measured SDAS show acceptable agreement (Fig. 5).

The micrograph section of the 16 mm step was taken in the cross section of the plate which is marked with an arrow in Fig. 8(a). Due to the initial composition of the alloy the precipitation of the phase Mg_2Si is expected. This phase is important for the adjacent heat treatment process (solutionizi quenching, aging). During solutionizing the temperature raised nearly to the eutectic temperature, which substanti dissolved the aforementioned alloying elements into so aluminium. During the so called aging the elements came of solution to form strengthening particles [13].

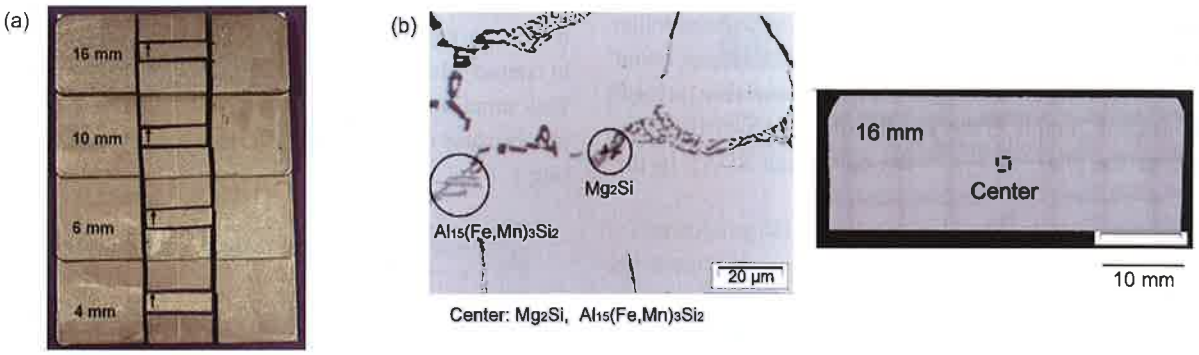

Fig. 8: (a) Position of metallographic samples for examination of grain size and precipitated phases; (b) Micrograph of 16 mm step showing intermetallic Mg_2Si and Fe-rich phases in the as-cast mircostructure

The simulated fraction of the Mg_2Si and the iron containing phases varied from 0.49% to 0.77% and 0.60% to 0.76%, respectively (Fig. 9 and Fig. 10). These aforementioned phases could be detected during optical light microscope examination (Fig. 8b). Horng et al. [14] investigated the fracture behaviour of A356 alloy which has a similar composition than the alloy used in this work. They varied the Fe-content within the range of 0.14wt.% – 0.97wt.%, and their results indicated that if the Fe-content is below 0.57wt.%, the Fe-rich intermetallic parti are mainly π-$Al_8Mg_3FeSi_6$ and α-$Al_{15}Fe_3Si_2$ phases [14-15]. As in this work the plate-like Fe-rich phase (β-AlFeSi) was observed. The fraction of the Mg_2Si and ferrous phases coul estimated by determining the area ratio of the respective ph This ratio is in both cases less than 1% which fits qualitati well to the simulation results.

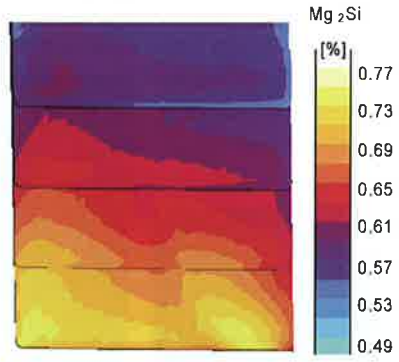

Fig. 9: Distribution of phase fraction of Mg_2Si resulting from simulation

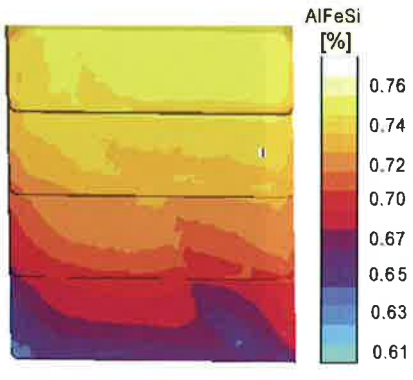

Fig. 10: Distribution of phase fraction of AlFeSi resulting from simulation

To determine the grain size in each of the four steps, sam were taken on the position shown in Fig. 8(a) and etched Barker (Fig. 11). The lengths of 68 grains were measure get information about the order of the grain size. It was fo that the maximum grain size is in the order of 0.86 mm the minimum 0.13 mm. The arithmetic mean value is 0.42 and the standard deviation 0.16 mm. After removal of 2 of the surface by grinding the grain size was analysed ag The maximum grain size of the second analysis is 0.84 and the minimum 0.15 mm. The arithmetic mean value is

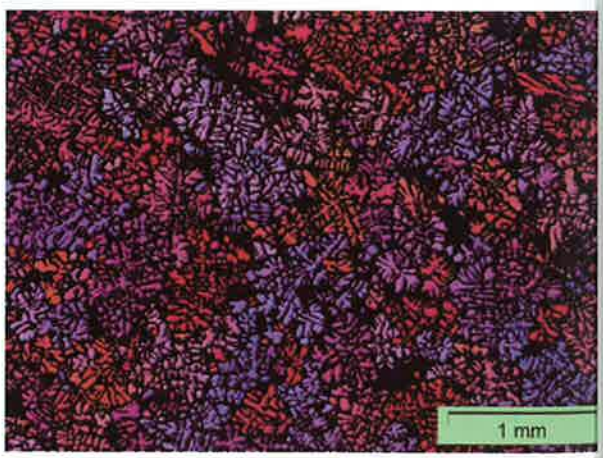

Fig. 11: Micrograph under polarized light after Barker's etching observed with light optical microscope (Shown are the grain contours of a sample taken in center of the 16 mm step after anodic oxidation)

mm and the number of measured grains was 71 mm. In Fig. 11 the contours of the grains are shown. Both simulation result and experimental measurement showed similar distribution behaviour of the grain size: a generally uniform grain size distribution in the whole casting, slightly increase of the grain size in the large section, which seems to fit to the theory. As we know that among many factors influencing the grain size in aluminium cast part, grain refiner plays a dominant role [12]. Experimental and numerical results verified that the cooling rate has only minor influence on the grain size.

In the current AlSi7MgCu0.5 alloy, the titanium content (0.11wt.%) serves as grain refiner. The simulation results show that the calculated grain size is overestimated by a factor of two compared to reality (Fig. 12). It is unclear at this moment whether this discrepancy is from the mother alloy for this experiment, which might be not properly prepared and controlled, or from the numerical model. For this further investigation is still required.

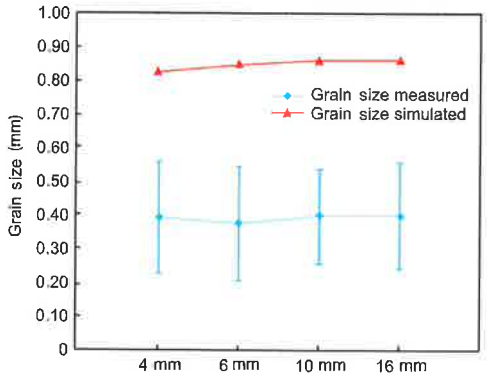

Fig. 12: Comparison of measured and simulated grain sizes in the four steps

3 Conclusions

The simulation results obtained with a commercial casting software like the temperature field, magnitude and distribution of the secondary dendrite arm spacing, grain size and the interdendritic phases of Mg_2Si and AlFeSi of an aluminium alloy were validated by comparison with experimental data. The following conclusions were drawn.

(1) By deriving the heat transfer coefficients (HTC's), as function of temperature but uniform in all casting sections, from measured temperature curves with a reverse calculation method, a close agreement in the thermal conditions between experiment and simulation was obtained in step 1 – 3. Some difference between measured and simulated temperature was found in step 4. This discrepancy indicates that a uniform HTC for all four steps might underestimate the cooling rate in the lower part of the casting section. And also the displacement due to shrinkage and the resulting gap between mould and casting was not taken into account.

(2) The simulated distribution of the SDAS showed an acceptable agreement with the experimental results. Both experiment and simulation showed a general SDAS distribution pattern: SDAS increases with the casting wall thickness; and the left hand side of the plate (away from the gating system) has relatively smaller SDAS than the right hand side (connecting to the gating system) due to the different cooling rates between the left and right sides. The strong variations of the experimental estimated SDAS within a step can be explained by the standard intercept count method. The observation of the SDAS was performed on planar sections through the material. Hence, the three dimensional dendrites were cut by a cutting plane and only the two dimensional features of the dendrites in the cross section were measured. This causes scattered measurement results.

(3) The interdendritic phases Mg_2Si and AlFeSi were identified by light microscopic examination. The prediction of the phase ratio on the metallographic sample was near the resolution limit of the microscope; hence it was not possible to quantify the area fraction. But it was possible to estimate the amount of both phases as less than one percent which fits quite well to the simulated amounts.

(4) The simulated grain size is about the factor of two larger than the grain size found by light microscopic examination. On the other hand, simulation results and experimental measurement showed that a generally uniform grain size distribution in the whole casting was found, and the cooling rate has only minor influence on the grain size. Reason for this demands further investigations, from both experimental and modelling aspects.

References

[1] Lee P D, Chirazi A, Atwood R C, Wang W. Multiscale Modelling of Solidification Microstructure and Microporosity in an Al-Si-Cu Alloy. Mater. Sci. Eng. A, 2004, 365: 57–65.

[2] Eskin D, Du Q, Ruvalcaba D, Katgerman L. Experimental Study of Structure Formation in Binary Al-Cu Alloys at Different Cooling Rates. Mater. Sci. Eng. A, 2005, 405: 1–10.

[3] Gowri S. Comparison of Thermal Analysis Parameters of 356 and 359 Alloy. AFS Trans., 1994, 102: 503–508.

[4] Ananthanarayanan L, Samuel F H, Gruzelski J. Thermal Analysis Studies on the Effect of Cooling Rate on the Microstructure of 319 Aluminum Alloy. AFS Trans., 1992, 100: 383–391.

[5] Shabestari S G, Malekan M. Thermal Analysis Study of the Effect of the Cooling Rate on the Microstructure and Solidification Parameters of 319 Aluminium Alloy. Canadian Metallurgical Quarterly, 2005, 44: 305–312.

[6] Kappey J, Fainberg J, Schneider M, et al. Microstructure, Defects and Properties in Aluminium Alloy Castings: Modelling and Simulation. In: Proc. 1st Conf. Multiphysics Simulation, published by Fraunhofer SCAI, Bonn, 2010 available on CD.

[7] Hasse S. Giesserei Lexikon. 18th ed. D-Berlin, Schiele u. Schön, 2000: 229.

[8] Brresi J, Kerr M J, Wang H, Couper M J. Effect of Magnesium, Iron and Cooling Rate on Mechanical Properties of Al-7Si-Mg Foundry Alloys. AFS Trans., 2000, 108: 563–570.

[9] Caceres C H, Wang Q G. Solidification Conditions, Heat Treatment and Tensile Ductility of Al-7Si-0.4Mg Casting Alloys. AFS Trans., 1996, 104: 1039–1043.

[10] Thorvaldsen A. The Intercept Method. Determination of Spatial Grain Size. Acta. Mater., 1997, 45, 595 – 600.

[11] Flemmings M C. Solidification Processing, McGraw-Hill, USA-

New York, 1974.
[12] Eskin D, Du Q, Ruvalcaba D, Katgerman L. Experimental Study of Structure Formation in Binary Al-Cu Alloys at Different Cooling Rates. Mater. Sci. Eng. A, 2005, 405: 1 – 10.
[13] Liscic B, Tensi H M, Canale L C F, Totten G E. Quenching Theory and Technology. 2nd ed., CRC Press, UK, 2010.
[14] Horng J H, Jiang D S, Lui T S, Chen L H. The Fracture Behaviour of A356 Alloys with Different Iron Contents under Resonant Vibration. Int. J. Cast Met. Res, 2000, 13, 215–222.
[15] Yi J Z, Gao Y X, Lee P D, Lindley T C. Effect of Fe-Content on Fatigue Crack Initiation and Propagation in a Cast Aluminium-Silicon Alloy (A356-T6). Mater. Sci. Eng. A, 2004, 386: 396 – 407.

This paper was financially supported by the Austrian Federal Government (in particular from the Bundesministerium für Verkehr, Innovation und Technologie and the Bundesministerium für Wirtschaft, Familie und Jugend) and the Styrian Provincial Government, represented by Österreichische Forschungsförderungsgesellschaft mbH and by Steirische Wirtschaftsförderungsgesellschaft mbH, within the research activities of the K2 Competence Centre on "Integrated Research in Materials, Processing and Product Engineering", operated by the Materials Center Leoben Forschung GmbH in the framework of the Austrian COMET Competence Centre Programme.